

Electronic stopping power in gold: The role of d electrons and the H/He anomaly

M. Ahsan Zeb,¹ J. Kohanoff,² D. Sánchez-Portal,^{3,4} A. Arnau,^{3,4,5} J. I. Juaristi,^{3,4,5} and Emilio Artacho^{1,6,7}

¹*Cavendish Laboratory, University of Cambridge, Cambridge CB3 0HE, United Kingdom*

²*Atomistic Simulation Centre, Queen's University, Belfast BT7 1NN, United Kingdom*

³*Centro de Física de Materiales CFM/MPC (CSIC-UPV/EHU), 20018 San Sebastián, Spain*

⁴*Donostia International Physics Center DIPC, Paseo Manuel de Lardizábal 4, 20018 San Sebastián, Spain*

⁵*Departamento de Física de Materiales, Facultad de Químicas, UPV/EHU, 20018 San Sebastián, Spain*

⁶*Nanogune and DIPC, Tolosa Hiribidea 76, 20018 San Sebastián, Spain*

⁷*Basque Foundation for Science, Ikerbasque, 48011 Bilbao, Spain*

(Dated: 6 May 2012)

The electronic stopping power of H and He moving through gold is obtained to high accuracy using time-evolving density-functional theory, thereby bringing usual first-principles accuracies into this kind of strongly coupled, continuum non-adiabatic processes in condensed matter. The two key unexplained features of what observed experimentally have been reproduced and understood: (i) The non-linear behaviour of stopping power versus velocity is a gradual crossover as excitations tail into the d -electron spectrum; and (ii) the low-velocity H/He anomaly (the relative stopping powers are contrary to established theory) is explained by the substantial involvement of the d electrons in the screening of the projectile even at the lowest velocities where the energy loss is generated by s -like electron-hole pair formation only.

Non-adiabatic processes are at the heart of aspects of science and technology as important as radiation damage of materials in the nuclear and space industries, and radiotherapy in medicine. Yet, in spite of a long history, the quantitative understanding of non-adiabatic processes in condensed matter and our ability to perform predictive theoretical simulations of processes coupling many adiabatic energy surfaces is very much behind what accomplished for adiabatic situations, for which first-principles calculations provide predictions of varied properties within a few percent accuracy. Substantial progress has been made for weakly non-adiabatic problems such as the chemistry of vibrationally excited molecules landing on metal surfaces [1], but not in the stronger coupling regime of radiation damage. Recently, the electronic stopping power for swift ions in gold has been carefully characterized by experiments [2–4], showing flagrant discrepancies with the established paradigm for such problems [5, 6], and only qualitative agreement with time-dependent tight-binding studies [7], and with detailed studies for protons based on first principles [8], leaving very fundamental questions unanswered in spite of the apparent simplicity of the system. Most notably the H/He anomaly: the present understanding predicts a stopping power for H higher than for He at low velocities [6], which strongly contradicts the recent experiments [4].

A particle moving through a solid material interacts with it and loses its kinetic energy to both the nuclei and the electrons inside it. At projectile velocities between 0.1 and 1 atomic units (a.u. henceforth) both the nuclear and the electronic contributions to the stopping power (energy lost by the projectile per unit length) are sizeable [7]. Based on the jellium model (homogeneous electron gas) the electronic stopping power, S_e , is predicted to be $S_e \propto v$ for a slow projectile traversing a

metallic medium [9, 10]. Such behaviour has been observed experimentally in many sp -bonded metals [11, 12], and the jellium model has allowed deep understanding of the dynamic screening of the projectile and its relation to stopping [13]. Even the jellium prediction of an oscillation of the proportionality coefficient with the projectile's atomic number Z has been verified [6] and reproduced by ab initio atomistic simulations [14]. However, phenomena that cannot be accounted for within the jellium paradigm have been described only qualitatively so far [15–18]. Experiments on noble metals Cu, Ag and Au, show pronounced nonlinearities in $S_e(v)$ [2–4, 8, 11, 15, 19]. In the case of slow H and He ions in gold [2–4], $S_e(v)$ displays an increase in the slope roughly around $v \simeq 0.18$ a.u. This is usually attributed to a threshold projectile velocity needed to excite the d -band electrons that are relatively tightly bound. A model was developed based on the ab initio density of electronic states and a stochastic treatment of excitations [17], which reproduces the threshold for protons. Here we obtain the non-linear $S_e(v)$ and the H/He anomaly with a general purpose ab initio method equally applicable to many other radiation problems.

We calculate the uptake of energy by the electrons in gold from a moving H or He ion in its $\langle 100 \rangle$ channel by explicitly following the dynamics of the electrons coupled to the projectile's motion, using time-evolving time-dependent density functional theory (TDDFT) [20]. We find very good quantitative agreement with some recent low energy ion scattering experiments on thin gold films [2–4]. The results are analyzed in terms of the electronic excitations that are responsible for the energy loss, which very clearly shows why the slope of S_e increases with projectile velocity. In contrast to the usual idea that at low projectile velocity only electrons close to the Fermi energy contribute to the stopping, we find that there is a

significant contribution from deep lying states even for a slow projectile. This means that at low velocities ($v < 0.2$ a.u.) the electrons accessible to excitations (s) are different from the ones involved in the screening of the projectile ($s+d$), the latter providing the excitation *mechanism*.

We performed all calculations using the SIESTA method [21] in its time evolving TDDFT implementation [22]. We used the Perdew-Burke-Ernzerhof (PBE) version [23] of the Generalised Gradient Approximation (GGA) to the instantaneous exchange and correlation functional. Since we are only interested in the very low energy regime that is far below core electrons excitation thresholds, only valence electrons in Au are considered explicitly and a norm-conserving pseudopotential is used to describe the core electrons (up to the $5p$ sub-shell). Further details are found in [24]. After placing the projectile in a $[001]$ channel and finding the DFT ground state, it is given an initial velocity along the z -direction while all gold atoms are initially quiescent. The system evolves by following Ehrenfest coupled electron-ion dynamics. On the time scale of the simulation ($\sim 0.75 - 6.0$ fs for $v = 0.05 - 0.50$ a.u.), the gold nuclei only gained negligible velocities and did not move significantly. We monitored the total energy of the electronic subsystem as a function of time. Once the transient related to the sudden start has disappeared [18, 24], S_e is extracted as the average rate of change of the electronic energy with the distance travelled by the projectile.

Fig. 1 shows our results for $S_e(v)$ for H and He projectiles in gold for the velocity range $v = 0.06 - 0.50$ a.u. We also plot results of some recent experiments performed on thin single crystal gold films oriented along $\langle 100 \rangle$ [2] and polycrystalline gold films [3, 4]. The agreement between our simulations and the experiments is noticeable. Although the stopping power is still underestimated (especially for H around $v = 0.3$ a.u.), no previous ab initio approach had this level of agreement on the non-linear velocity dependence of the stopping power of real materials. Our results for the stopping power are well converged with respect to the basis size and the density of points on the real and the momentum space grids [24]. A larger basis set for the projectile, however, (TZDP instead of DZP [24]) increases the stopping power about 5% at $v = 0.5$ a.u., but considerably less at low velocity. The error bars in Fig. 1 indicate the dispersion in our results for $v = 0.08, 0.1$ and 0.5 a.u. when the various parameters are varied, including the basis set [24] (the bars for low velocities are hardly larger than the size of the circles). The strict channelling in the simulation is partly behind the observed underestimation: calculations for a 30% smaller impact parameter give a 25% increase in S_e^{H} at $v = 0.28$ a.u. that reduces to 1% at $v = 0.5$ a.u.

We see a clear deviation from the linear behaviour around $v = 0.2$ a.u. in S_e of both H and He. This is unlike the $S_e \propto v$ of the uniform electron gas. It seems a plausible explanation that at low projectile velocity only

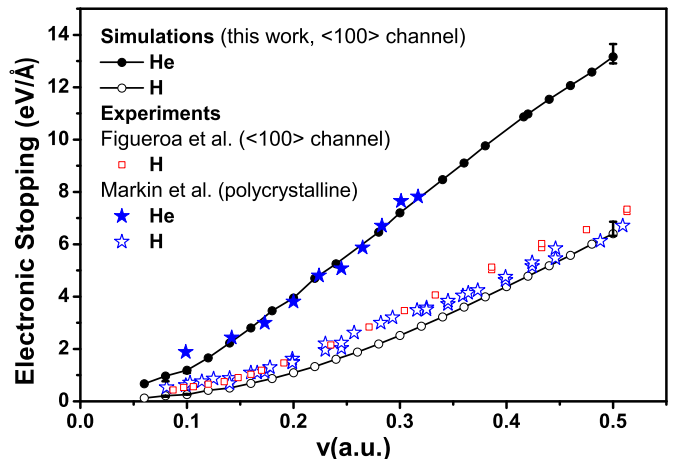


FIG. 1. Electronic stopping power of H and He projectiles in gold as a function of projectile velocity. Results of our simulations are compared with the experimental data from Refs. [2–4] on single and polycrystalline thin gold films.

s -band electrons from the states around the Fermi energy contribute to the stopping and at higher velocity electrons in the d band that lie relatively deeper in energy are also able to take part in it, resulting in an increase in the slope of S_e . Thus, comparisons have been made [2, 4] with jellium using the average electron density n_e of the s electrons ($r_s = 3.01$ a.u., where $n_e^{-1} = \frac{4}{3}\pi r_s^3$), using $r_s = 1.49$ a.u., corresponding to an effective number of s and d electrons [4], or of the density in the $\langle 100 \rangle$ channel ($r_s = 1.8$ a.u.). However, the jellium predictions do not agree with the experimental results except at projectile velocities around $v = 0.6$ a.u. in the latter case, despite the expectation that all the d -band electrons are active for a projectile velocity $v \geq 0.47$ a.u. [15]. There is a further problem in the comparison with jellium: If we assume that at low velocity only s electrons are actively participating in the stopping mechanism, the jellium model predicts $S_e^{\text{H}} > S_e^{\text{He}}$ [5], which is not the case.

To explain the above inconsistencies and get a better idea of the energy loss mechanism we compute the changes in the electronic distribution due to the excitation of the electrons when a projectile propagates through the material. Having $\{\psi_n(t)\}$ and $\mathbf{X}(t)$, the set of evolved occupied KS states, and the corresponding atomic positions at time t , we calculate the adiabatic states $\{|\phi_i, \mathbf{X}\rangle\}$, i.e., the set of self-consistent static KS states for $\mathbf{X}(t)$. By projecting the evolved states onto the adiabatic states, $C_{in} = \langle \phi_i, \mathbf{X}(t) | \psi_n(t) \rangle$, the density of occupied energy states $O(E)$ at time t as a function of energy E are obtained as $O(E) = \sum_{i,n} |C_{in}|^2 \delta(E - E_i)$. Here E_i is the eigenvalue of the adiabatic state $|\phi_i, \mathbf{X}\rangle$. To compute the change in the electronic distribution or the (electron-hole) excitation distribution, $P(E)$, we subtract the ground state electronic distribution from $O(E)$.

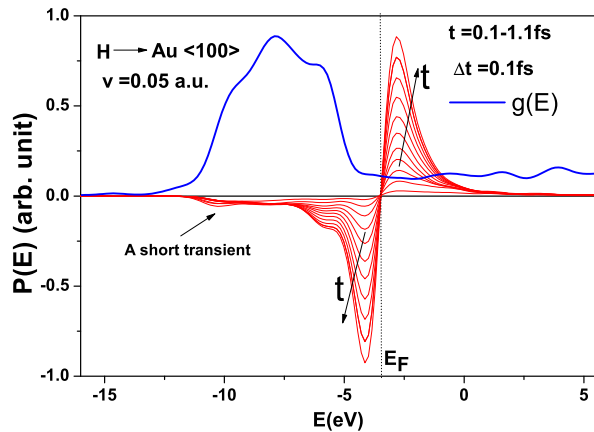


FIG. 2. (Color online) Excitation distribution $P(E)$ when H passes through gold with velocity 0.05 a.u., for time values between $t = 0.1$ fs and 1.1 fs in steps of $\Delta t = 0.1$ fs (light color; larger amplitude for longer t ; Gaussian broadening $\sigma = 0.2$ eV). The dark curve is the electronic density of states $g(E)$ ($\sigma = 0.5$ eV). $P(E)$ and $g(E)$ are in different scales.

That is, $P(E) = O(E) - \Theta(E_F - E)g(E)$, where E_F is the Fermi energy of the system, $g(E)$ is the electronic density of states and $\Theta(E)$ is the Heaviside step function.

Fig. 2 shows the excitation distribution $P(E)$ as a function of energy at various instants from $t = 0.1$ fs to $t = 1.1$ fs with an interval $\Delta t = 0.1$ fs, for the passage of a H atom in gold along $\langle 100 \rangle$ with velocity $v = 0.05$ a.u. The electronic density of states of the bulk Au host $g(E)$ is also plotted in Fig. 2. The negative and the positive values of $P(E)$ show the density of empty and filled states below and above E_F , respectively, due to the electronic excitations caused by the moving projectile. Notice that despite being very slow ($v = 0.05$ a.u.), the projectile is able to excite relatively tightly bound d -band electrons. A short initial transient behaviour is noticeable in Fig. 2: at energies deep below the Fermi energy, the number of empty states becomes larger initially, requiring a short time to adjust to a stationary regime. This is because in our simulations the projectile is a static impurity atom at $t = 0$ that suddenly acquires a finite velocity resulting in a large initial perturbation.

To see how the excitation distribution after the transient depends on the velocity of the projectile, we plot $P(E)$ against E in Fig. 3 at $t = 0.25$ fs for various projectile velocities, between 0.05 a.u. and 0.50 a.u. We see that, compared to the states just below the Fermi energy, the number of excitations from deep inside the d -band increases more quickly with the velocity of the projectile. This means that the effective number of d -band electrons involved directly in excitations provoking the stopping process increases with the projectile velocity. To see this more clearly, we separated the energy window into two parts at the upper edge of the d -band at energy E_d and

calculated the total number of excitations N_1 and N_2 from the states below and above E_d for a constant distance travelled by the projectile. We find that $P(E) \propto t$ after the initial transient so we can estimate N_1 and N_2 as $N_1 = \frac{1}{v} \int_{-\infty}^{E_d} |P(E)| dE$ and $N_2 = \frac{1}{v} \int_{E_d}^{E_F} |P(E)| dE$, which we did using $P(E)$ at $t = 0.25$ fs. In the inset of Fig. 3 we plot N_1 and N_2 and the fraction $N_1/(N_1 + N_2) = N_1/N$ against the projectile velocity as dashed, dotted and solid lines for H and He projectiles. We see that N_1 and N_1/N increase with v for both projectiles. For H, N_2 increases and saturates whereas for He it increases up to $v = 0.3$ a.u. but decreases for a faster projectile. Since there is one s electron and ten d electrons and N_1 also includes the contribution from the s -band states, ideally it should tend to $N_1/N \sim 10/11 = 0.909$ for high projectile velocity. N_1/N reaches only 0.88 and 0.78 for H and He at $v = 0.5$ a.u. Although the fraction of excitations from the deep lying states is higher for H, the absolute number

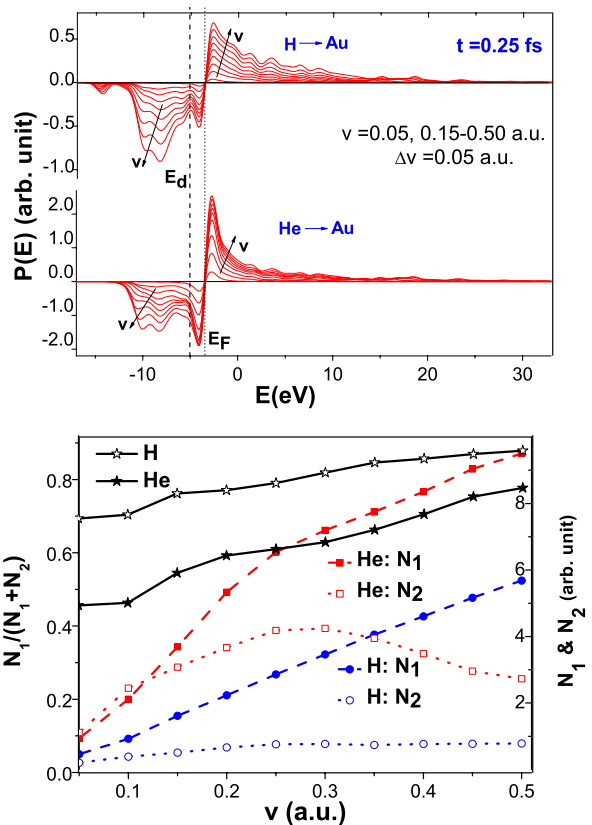


FIG. 3. Up: Excitation distribution $P(E)$ due to the passage of a H (top) or He projectile (bottom) in gold evaluated at $t = 0.25$ fs for various projectile velocities, $v = 0.05 - 0.50$ a.u. in steps of 0.05 a.u. Increased projectile velocity gives curve with larger amplitude (indicated by arrows). The dashed and dotted vertical lines show the upper edge of the gold's $5d$ -band E_d and the Fermi energy E_F . Down: Number of empty states below and above E_d , N_1 and N_2 , and fraction $N_1/(N_1 + N_2)$ versus projectile velocity, due to the excitations for H or He.

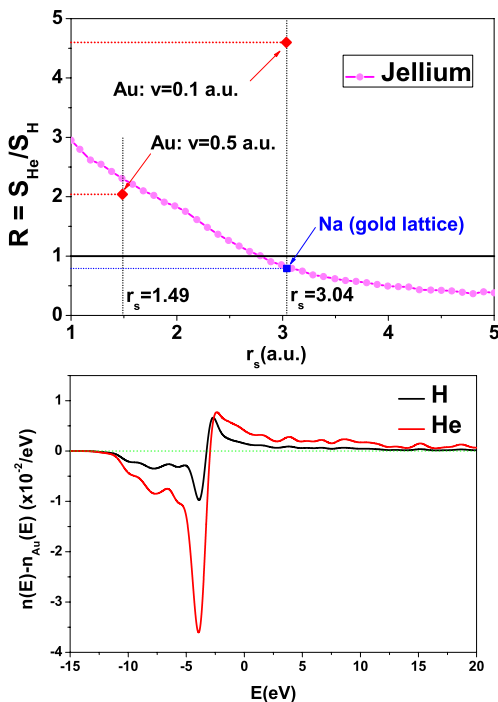


FIG. 4. Up: The curve shows $R = S_e^{\text{He}}/S_e^{\text{H}}$ for jellium versus the electron density parameter r_s [5]. The values of R obtained for Au for $v = 0.1$ and 0.5 a.u. are associated with $r_s = 3.04$ and 1.49 a.u., respectively, following Ref. [4]. The calculated ratio R for a system made of Na atoms in bulk Au positions, $r_s = 3.04$, is also presented. Down: Projection of KS states for the system with projectile onto the KS states of bulk Au, for H and He, subtracting the Au density of states.

is lower, as can be seen in the figure. Furthermore, in the case of H, $N_1 > N_2$ for the whole velocity range shown whereas for He, $N_2 > N_1$ in the very low velocity range.

We address now the low-velocity H/He anomaly. Fig. 4 presents the ratio $R = S_e^{\text{He}}/S_e^{\text{H}}$ in jellium [5]. The values of R for Au for $v = 0.1$ and $v = 0.5$ a.u. are plotted on the two dotted vertical lines at $r_s = 3.04$ and $r_s = 1.49$ a.u., which correspond to 1 and 8.24 electrons per bulk unit cell, i.e., the s electrons and the effective number of valence electrons (s and d) that fit the plasmon pole for bulk Au [4]. We see that for the faster projectile R is close to the jellium value and significantly larger than 1. However, for the slower one, we obtain $R = 4.7$, in clear disagreement with the jellium value of 0.79, but in agreement with experiment. We also plot R for the fictitious system built by putting Na atoms in the Au positions, which corresponds to an electron gas with $r_s = 3.04$. The plot shows a perfect agreement for the R values of Na and jellium [25]. These differences between jellium (or Na) and gold are thus due to the presence of gold's d electrons. This is consistent with the fact that, even if a slow projectile were unable to excite the d -band electrons appreciably, the presence of the projec-

tile in gold constitutes a large static perturbation for the d electrons. This can be clearly seen by calculating the projection of the ground state of the gold with the projectile onto that without it and obtaining a distribution analogous to $P(E)$, now describing the static screening of the projectile. i.e., projecting the wave-functions of Au with the projectile onto the states of pure Au (Fig. 4). This means that for a slow projectile the response of the electrons in gold is far from the one described by the homogeneous electron gas model that includes just the s -band electrons.

To summarize, we have shown that realistic non-adiabatic stopping of projectiles in real metals can now be described from first-principles with acceptable accuracy, even at the Ehrenfest dynamics level. We used it to calculate the electronic energy loss on passage of H and He through Au and find good quantitative agreement with experiments. Many problems can now be addressed with this technique in the fields mentioned in the introduction.

JK thanks the Wellcome Trust for a Flexible Travel award. MAZ acknowledges support of the Islamic Development Bank. DSP, JIJ and AA acknowledge support of the University of the Basque Country UPV/EHU, under Grant IT-366-07, and of the Spanish Ministerio de Ciencia e Innovación under Grant FIS2010-19609-C02-00. The calculations were done using the CamGrid high-throughput facility of the University of Cambridge.

-
- [1] N. Shenvi, S. Roy and J. C. Tully, and refs. therein, Science **326**, 829 (2009).
 - [2] E. A. Figueroa, E. D. Cantero, J. C. Eckardt, G. H. Lantschner, J. E. Valdés, and N. R. Arista, Phys. Rev. A **75**, 010901 (2007).
 - [3] S. N. Markin, D. Primetzhofer, S. Prusa, M. Brunmayr, G. Kowarik, F. Aumayr, and P. Bauer, Phys. Rev. B **78**, 195122 (2008).
 - [4] S. N. Markin, D. Primetzhofer, M. Spitz, and P. Bauer, Phys. Rev. B **80**, 205105 (2009).
 - [5] P. M. Echenique, R. M. Nieminen and R. H. Ritchie, Solid State Comm. **37**, 779 (1981).
 - [6] P. M. Echenique, F. Flores and R.H. Ritchie, Solid State Physics **43**, eds. H. Ehrenreich and D. Turnbull, Academic Press, p. 230 (1990).
 - [7] C. P. Race, D. R. Mason, M. W. Finnis, W. M. C. Foulkes, A. P. Horsfield, and A. P. Sutton, Rep. Prog. Phys. **73**, 116501 (2010), and refs. therein.
 - [8] E. D. Cantero, G. H. Lantschner, J. C. Eckardt, and N. R. Arista, Phys. Rev. A **80**, 032904 (2009).
 - [9] R. H. Ritchie, Phys. Rev. **114**, 644 (1959).
 - [10] M. Kitagawa and Y. H. Ohtsuki, Phys. Rev. B **9**, 4719 (1974).
 - [11] J. E. Valdés and G. Martínez-Tamayo, G. H. Lantschner, J. C. Eckardt and N. R. Arista, Nucl. Instrum. Meth. B **73**, 313 (1993).
 - [12] G. Martínez-Tamayo, J. C. Eckardt, G. H. Lantschner, and N. R. Arista, Phys. Rev. A **54**, 3131 (1996).
 - [13] M. Quijada, A. G. Borisov, I. Nagy, R. Díez Muiño, and

- P. M. Echenique, Phys. Rev. A **75**, 042902 (2007).
- [14] R. Hatcher, M. Beck, A. Tackett, and S. T. Pantelides, Phys. Rev. Lett. **100**, 103201 (2008).
- [15] J. E. Valdés, J. C. Eckardt, G. H. Lantschner, and N. R. Arista, Phys. Rev. A **49**, 1083 (1994).
- [16] P. Vargas, J. E. Valdés and N. R. Arista, Phys. Rev. A **53**, 1638 (1996).
- [17] J. E. Valdés, P. Vargas and N. R. Arista, Phys. Rev. A **56**, 4781 (1997).
- [18] J. M. Pruneda *et al.* Phys. Rev. Lett. **99**, 235501 (2007).
- [19] R. Blume, W. Eckstein, and H. Verbeek, Nucl. Instrum. Methods **168**, 57 (1980); **194**, 67 (1982).
- [20] E. Runge and E. K. U. Gross, Phys. Rev. Lett. **52**, 997 (1984).
- [21] P. Ordejón, E. Artacho, and J. M. Soler, Phys. Rev. B **53**, 10441 (1996); J. M. Soler *et al.*, J. Phys. Condens. Matter **14**, 2745 (2002).
- [22] A. Tsolakidis, D. Sánchez-Portal, and R. M. Martin, Phys. Rev. B **66**, 235416 (2002).
- [23] J. P. Perdew, K. Burke and M. Ernzerhof, Phys. Rev. Lett. **77**, 3865 (1996).
- [24] See details in supplementary materials.
- [25] The stopping power values for H and He in this Na are 3.902 eV/Å and 3.083 eV/Å, respectively, for $v = 0.5$ a.u., and 1.024 eV/Å and 0.715 eV/Å, for $v = 0.1$ a.u.; the corresponding values for jellium as extracted from Ref. [5] are 7.741 eV/Å and 17.874 eV/Å, respectively, for $v = 0.5$ a.u., and $r_s = 1.49$ Bohr; and 0.861 eV/Å and 0.710 eV/Å, for $v = 0.1$ a.u. and $r_s = 3.04$ Bohr.